Spin-Lattice Relaxation and Rotational Motion of Aromatic Triplet-State Molecules in Supercooled Alkane Solvents (Part 1)†

Albert A. Ruth*

Department of Physics, National University of Ireland, University College Cork, Cork, Ireland

Bernhard Nickel‡

Max-Planck-Institut für Biophysikalische Chemie, Abteilung Spektroskopie und Photochemische Kinetik, Am Fassberg, D-37077 Göttingen, Germany

Received: August 13, 2005; In Final Form: August 26, 2005

The phosphorescence of phenazine (PZ) and quinoxaline (QX) was investigated after pulsed laser excitation in the glass-transition range of several alkane solvents. Three relaxation processes of PZ and QX in the metastable triplet state, T_1, were studied as a function of temperature: (1) the decay of the selective population of the strongly phosphorescent triplet substate T_{1x} due to spin-lattice relaxation (SLR), (2) the time-dependent red shift of the phosphorescence spectrum due to the solvation of triplet-state molecules, and (3) the decay of the phosphorescence polarization due to orientational relaxation (OR). Various aspects and connections of the mechanisms governing the three relaxation phenomena are discussed. The relaxation dynamics were characterized at temperatures above the glass-transition temperature of the respective solvent, where the fundamental processes involved are strongly dependent upon the solvent viscosities. For the systems treated here, OR and solvation were satisfactorily described by a Vogel−Fulcher−Tammann temperature behavior. SLR also depends on properties of the alkane solvent above the glass transition. Upon cooling, SLR becomes independent of the specific solvent properties and is based on mechanisms that are typical for amorphous glasses or solids. (This particular aspect will be the subject of a subsequent publication, part 2).

1. Introduction

Investigations on organic molecules in their metastable triplet state (T_1) using methods of magnetic resonance are highly restricted in *fluid* solution as a result of fast spin-lattice relaxation (SLR).[1] The rotational motion of triplet-state molecules causes very effective spin relaxation even in *viscous* solution. An exact correlation between SLR and the coupling of aromatic triplet-state molecules to their molecular environment in solution, which is based on rotational diffusion and solvation dynamics, has not yet been found. To study the connection between SLR and orientational relaxation (OR) in highly viscous solution, we previously investigated the time-dependent phosphorescence of phenazine (PZ) in the glass-transition range of two alkane solvents.[2] SLR in the triplet state of PZ leads to an initial change in the phosphorescence intensity from which an effective rate coefficient, k_s, for SLR can be deduced.[2−7] The rate coefficient k_r for OR can be obtained from the dynamics of the phosphorescence depolarization.[8−10] The original expectation at the start of the work in ref 2 was that, in a sufficiently viscous solvent at low temperatures, SLR and OR could be observed simultaneously. To find a relationship between SLR and OR, two similar glass-forming solvents (sol) with significantly different glass-transition temperatures, T_g, were used. We expected that in the glass-transition range, where the viscosities of the two solvents obey $\eta^{sol1} > \eta^{sol2}$, both of the effective rate coefficients k_s and k_r would obey the following relationships, $k_s^{sol1} < k_s^{sol2}$ and $k_r^{sol1} < k_r^{sol2}$, and that a simple correlation between the differences $k_s^{sol1} - k_s^{sol2}$ and $k_r^{sol1} - k_r^{sol2}$ could be found. However, it turned out that this expectation was much too optimistic, because the effective SLR rates were found to be more than 3 orders of magnitude greater than OR rates ($k_s \gg k_r$) at a given temperature.[2] In fact, in the glass-transition range, two processes contribute to SLR: (a) a thermally activated process (SLR_h) dominating SLR at higher temperatures in viscous solution, well above the glass-transition temperature, and (b) a process (SLR_l) that is active at low temperatures, where the solvent forms a hard amorphous glass.

The present investigation is part 1 of a continuation of the work in ref 2 and will deal with the following issues, which have not been addressed previously:

(A) In ref 2, the hypothesis was made that the high-temperature SLR mechanism is solvent-dependent, whereas the low-temperature mechanism of SLR (SLR_l) should be virtually independent of the solvent. To verify this prediction, SLR rate coefficients of triplet PZ were systematically measured over a much wider temperature range and in several glass-forming alkane solvents. Additional measurements performed with quinoxaline (QX) in 3-methylpentane (3MP) will also enable a better interpretation of the data obtained previously.[2] These measurements will be presented in sections 3.2 and 3.2.1.

(B) In section 3.2.2, we will show that optical spin polarization (OSP), that is, strongly selective intersystem crossing (ISC) $S_1 \rightsquigarrow T_1$ from the lowest excited singlet state S_1 to the three triplet substates T_{1i} ($i = x, y, z$) of the metastable triplet state T_1, is independent of the excitation wavelength.

(C) The temperature dependence of OR was insufficiently addressed in ref 2 due to a lack of measurements at different

† Part of the special issue "Jürgen Troe Festschrift".

* Corresponding author. E-mail: a.ruth@ucc.ie.

‡ Passed away on January 27, 2002.

10.1021/jp0545546 CCC: $33.50 © 2006 American Chemical Society
Published on Web 10/26/2005

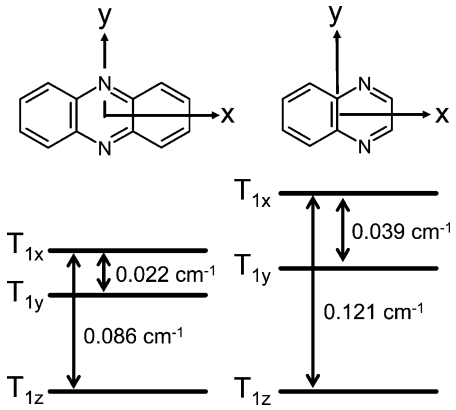

Figure 1. Left: triplet substates of PZ in a biphenyl host crystal at 1.2 K from ref 4. Right: triplet substates of QX in a durene host crystal at 1.24 K from ref 27. The *z* axis of the molecule's coordinate system runs perpendicular to the molecular plane. In state T_{1i}, the component S_i of the total spin is zero.

temperatures. The viscosity of the glass-forming solvents used was not known at the temperatures where OR times were measured. As a result of new viscosity data, measured at even lower temperatures using a falling-ball viscosimeter,[11] a quantitative evaluation of OR rates is possible and will be discussed in section 3.3.

(D) For probe molecules in highly viscous/glassy solvents, the solvation dynamics of the triplet state must also be considered in investigations of the time-dependent phosphorescence, because solvation occurs on a time scale that is relevant for the observation of OR and SLR. In ref 2, the solvation of triplet molecules was only treated in the form of an *effective* rate coefficient, k_e, of the molecular environment relaxation (MER). Even though the treatment of k_e bears useful empirical character, as will be shown in this paper, measurements of time-resolved phosphorescence spectra of PZ in 2,3-dimethylpentane (2,3DMP) will be presented in section 3.4 and discussed on the basis of triplet solvation.[12,13]

In part 2,[14] measurements of the phosphorescence of PZ and QX at temperatures below T_g will be presented to discuss SLR_l in disordered alkane glasses. Our previous work[2] was not conclusive as to whether SLR_l is better described by a thermally activated process or by a power law. In part 2, different models for the temperature dependence of SLR_l down to $T = 20$ K will be discussed.

1.1. Phosphorescence Kinetics. Apart from the normal triplet decay described by the rate constant $k_0 \approx (1/3)\Sigma_i k_i$ (where $k_i = k_{i,rad} + k_{i,nrad}$ is the rate coefficient for the radiative and nonradiative decay of the individual triplet substate T_{1i}, with $i = x, y$, and z; see Figure 1), the time dependence of the phosphorescence of aromatic compounds after photo-excitation is in general affected by three different relaxation processes: SLR, OR, and the solvation of the excited triplet which we will also refer to as MER. The time dependence of the phosphorescence intensity, $I(t)$, can be represented by

$$I(t) = I_0 \exp(-k_0 t)\, f_s(t)\, f_r(\delta,\kappa,t)\, f_e(\lambda,t) \qquad (1)$$

provided SLR is much faster than the decay of each triplet substate and MER does not change the total triplet decay (abbreviations and notations are in accordance with those in ref 2). Besides the total triplet decay[15] described by $\exp(-k_0 t)$ in eq 1, the three time-dependent factors, f_i (i = s, r, e), account for SLR (f_s), OR (f_r), and MER (f_e); if SLR, OR, and MER are much faster than the overall triplet decay, then I_0 simply represents the phosphorescence intensity immediately after excitation (at $t = 0$). The most important kinetic aspects of the three relaxation processes for this study are briefly outlined in the following (for a more detailed description of the kinetics, cf. section 2 in ref 2):

TABLE 1: Triplet Substate Parameters of PZ in a Biphenyl Crystal[4,17] at 1.2 K and of QX in a Durol Host Matrix[27,28] at 1.24 K[a]

solvent	T_{1i}	p_{i0}	$k_{i,rad}/k_{x,rad}$	k_i (s^{-1})
PZ	T_{1x}	0.9625	1.000	200
	T_{1y}	0.0106	0.020	14
	T_{1z}	0.0269	0.020	7
QX	T_{1x}	0.9551	1.000	11.1
	T_{1y}	0.0210	0.020	0.59
	T_{1z}	0.0239	0.015	0.40

[a] Primary probabilities, p_{i0}, of the population of T_{1i} were calculated from P_i in refs 4 and 27 using $p_{i0} = P_i/\Sigma_i P_i$. To avoid rounding errors, we are using more figures for p_{i0} than given for P_i in the literature.

Spin-Lattice Relaxation (f_s). Organic compounds that exhibit strong OSP[16] are particularly suitable for the determination of SLR rate coefficients. Because OSP creates nonequilibrium concentrations of the three triplet substates upon pulsed excitation, no resonant microwave field is necessary to saturate one of the triplet-substate transitions $T_{1i} \rightsquigarrow T_{1j}$ ($i, j = x, y, z$). At sufficiently high temperatures ($T > 20$ K) SLR is fast compared to the total triplet lifetime $\tau_0 = 1/k_0$ and, therefore, leads to a Boltzmann equilibrium in the population of the triplet substates. Thus, effective SLR rate coefficients (k_s) can be determined by monitoring the initial change in the intensity of the phosphorescence decay, which is obviously also dependent upon the individual radiative constants ($k_{i,rad}$) of each substate T_{1i}. The factor f_s in eq 1 takes the following form:

$$f_s(t) = 1 + \left[\frac{\Sigma_{i=1}^{3}(3p_{i0} - 1)k_{i,rad}}{\Sigma_{i=1}^{3}k_{i,rad}}\right]\exp(-k_s t) \qquad (2)$$

where p_{i0} is the relative probability of the population of T_{1i} by OSP ($\Sigma_i p_{i0} = 1$) and $k_{i,rad}$ is the rate coefficient of the radiative decay of T_{1i} (see Table 1). k_s is the effective rate coefficient of SLR, which is dependent on the individual SLR rate constants w_{ij} of the transitions $T_{1i} \rightsquigarrow T_{1j}$ ($i, j = x, y, z$). The relation between k_s and w_{ij} will be treated in part 2.[14]

The two compounds, PZ and QX, are two particularly suitable compounds for SLR measurements as a result of their photophysical properties, which comprise not only strongly selective ISC (either substate T_{1x} is populated with a probability of >95%)[3,4,17] but also large differences in the radiative decay of their triplet substates ($k_{x,rad}/k_{i,rad} < 0.005$; $i = y, z$). The photophysical properties of the triplet substates of PZ and QX are summarized in Table 1 and Figure 1.

Orientational Relaxation (f_r). Upon excitation with linearly polarized light, OR can be observed by monitoring the decay of the phosphorescence polarization. The phosphorescence depolarization is a measure of the slow rotational diffusion of molecules in a viscous solution. For molecules having at least one two-folded axis (point groups D_{2h} and C_{2v} in the case of PZ and QX, respectively), OR can be described by two exponentials.[18] Moreover, if the shape of the solute molecule can be approximated by a rotational ellipsoid and when at least one of the two transitions involved is polarized in the direction of the rotational axis of the ellipsoid, OR can be represented with sufficient accuracy with only a single exponential,[19,20] $\rho(t) = \exp(-k_r t)$, where k_r is the rate coefficient for OR. For the two compounds investigated here, this is the case (see section

3.3), and the factor f_r in eq 1 takes the form

$$f_r(\delta,\kappa,t) = 1 + (4/5)P_2(\cos\delta)\,P_2(\cos\kappa)\,\rho(t) \qquad (3)$$

with $P_2(\cos\xi) = (1/2)[3\cos^2(\xi) - 1]$, ($\xi = \delta, \kappa$).[21,22] δ is the angle between the emitting and the absorbing transition dipole in a solute molecule, and κ is the angle between the polarization directions of the excitation light and the luminescence detection beam. For $\kappa = 54.7°$ (magic angle polarization effects are eliminated at this angle),[22] $\kappa = 90°$, and $\kappa = 0°$, we will use the notation for the corresponding intensities $I_{mag}(t)$, $I_\perp(t)$, and $I_{||}(t)$, respectively.

Solvation (MER, f_e). Immediately after photo-excitation, the changed interaction between solute molecules and their molecular environment initiates a relaxation of the surrounding solvent molecules into a new equilibrium. This relaxation is due to the changed dipole and multipole moments of the solute in the initially excited Franck−Condon state compared to those in the electronic ground state. Environmental adjustments lower the energy of the excited state of the solute after excitation. This process of solvation can be observed spectroscopically as a time-dependent red shift of the phosphorescence spectrum with nonexponential behavior.[23] For nonpolar aprotic solvents such as the ones considered here, the red shift is generally small (<100 cm^{-1}).[12] Nevertheless, because the time scale on which solvation takes place can interfere with the measurements of OR and SLR, it needs to be considered. If the spectral resolution of the experimental setup at the detection wavelength is significantly higher than the width of the spectral features in the phosphorescence spectrum, the dynamical red shift of the spectrum can lead to an increase or decrease of the time-dependent phosphorescence intensity. An increase or decrease is observed if the wavelength-dependent phosphorescence spectrum has a negative or positive slope at the detection wavelength, respectively. In general, the solvation dynamics is characterized by a strongly nonexponential time dependence;[12,13] however, the increase or decrease in the phosphorescence intensity can be empirically described by a single exponential and, hence, an *effective* solvation time $\tau_e = 1/k_e$. The factor f_e in eq 1 takes the form

$$f_e(\lambda,t) = 1 + m(\lambda)\exp(-k_e t) \qquad (4)$$

where λ is the observation wavelength. The pre-exponential factor $m(\lambda)$ can have either a positive or a negative sign. It should be noted that describing the effect of solvation on the phosphorescence by a single exponential in eq 4 is a profound simplification. The *effective* rate constant k_e is only a relative measure for the dynamics of the solvation process; its absolute value cannot be easily associated with a physically relevant relaxation time scale. The application of eq 4 is only justified in an appropriate temperature range on the basis of its good empirical functionality. f_e will only be evaluated here to a have a simple way of comparing the temperature dependence of OR and SLR with MER (= solvation).

Being able to observe the three relaxation processes separately depends on the experimental conditions, which will be specifically outlined for each measurement. The effect of OR can be eliminated by measuring $I_{mag}(t)$, which causes $f_r(\delta,\kappa,t) = 1$ in eq 1. The effect of MER on the time dependence of the phosphorescence becomes negligible if a sufficiently broad interference filter (full width at half-maximum > 10 nm) is used in the detection beam instead of a high-resolution monochromator. This causes $m(\lambda)$ to be effectively 0 and, thus, $f_e(\lambda,t) = 1$ in eq 1. A further simplification of $I(t)$ results from the different order of magnitudes of the three relaxation-rate coefficients, k_s, k_e, and k_0, in the glass-transition range of a solvent. At temperatures where in principle all relaxation processes can have an effect on $I(t)$, the relation $k_s \gg k_e \gg k_0$ holds. Due to this fact, $I(t)$ could sufficiently accurately be described by only two exponentials in the glass-transition range of the alkanes in this study.

2. Experiment

Apparatus. The apparatus used to measure phosphorescence spectra and decays is essentially identical with that described in ref 2, except for two components:

(1) The nitrogen laser as the excitation light source was replaced by a dye laser (Lambda Physik F1-2000; DMQ, 365 nm) pumped by an excimer laser (Lambda Physik EMG-50; XeCl, 308 nm). The dye laser was used for the excitation of PZ; alternatively, only the excimer laser was used for the excitation of QX.

(2) Instead of the previously used nitrogen-flow cryostat, a new home-built cryostat was employed. With the new cryostat it was possible to cool the sample to a temperature as low as 20 K by using liquid helium as the coolant. The temperature of the sample was kept constant, within ±0.02 K above 70 K and within ±0.1 K at lower temperatures. The absolute temperature was measured with an accuracy of ±0.02 K (with a calibrated Pt-103 resistor in combination with a temperature controller, Lake Shore 330-Autotuning). Photodegradation of the sample was avoided by moving the cuvette relative to the excitation beam, as previously described.[2,24]

A red-sensitive photomultiplier tube (EMI 9558Q, S20) was used for all experiments. For the measurements of the time-dependent spectra presented in section 3.4, the tube was operated in connection with a fast delay (time range 3 μs−1 s) and gate (width 10 μs−1 s), or a gateable diode array (OSMA, Princeton Instruments) was used.

Samples. The samples were solutions of zone-refined PZ in different alkane solvents: 3MP, 2,3DMP, and the two 1:1 mixtures by volume of 3-methylpentane/isopentane (3MP/IP) and methylcyclohexane/methylcyclopentane (MCH/MCP). Zone-refined QX was only investigated in 3MP. The sample concentrations were typically between 2×10^{-5} and 10×10^{-5} M. All alkanes were fractionally distilled over a 1-m column, chromatographically purified, and dried with basic aluminum oxide. Traces of water were removed by means of a sodium/lead alloy (1:9) in 3MP for the preparation of the QX solutions. The sample preparation of the PZ solutions is described in detail in ref 2; for QX, only step 1 of the published procedure is different. While a concentrated solution of PZ was filled directly into a degassing bulb of a fluorescence cuvette, QX was first sublimed at 15 °C from a storage flask into a container with a well-defined volume to establish the right amount of substance. From there it was sublimed into the cooled degassing bulb (also cf. ref 25, p 23). This exploitation of QX's high vapor pressure additionally improves the purity of QX.

3. Results and Discussion

3.1. Phosphorescence Properties of PZ and QX. The absorption, the phosphorescence, and the polarization spectrum of PZ and QX in 3MP are shown in Figure 2.

Phenazine. From the phosphorescence decay of PZ in 3MP on a millisecond scale, a total triplet lifetime of $\tau_{0,pz} = 1/k_{0,pz} = 12.6 \pm 0.1$ ms was found, which agrees well with the average lifetime $\langle k_i\rangle^{-1} = 13.5$ ms, calculated with the values for k_i given in Table 1. With the exception of the measurements presented

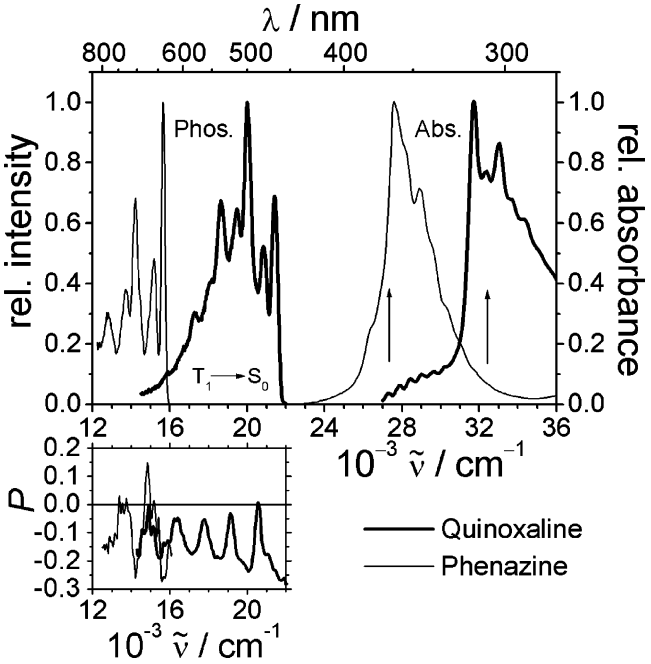

Figure 2. Corrected spectra of the phosphorescence (left) and the polarization degree (bottom left viewgraph) of PZ (thin lines) at T = 84.8 K and QX (thick lines) at T = 80 K. The corresponding absorption spectra (right) are measured at room temperature. The solvent was 3MP for all spectra. Vertical arrows indicate the excitation wavelengths at 365 and 308 nm for PZ and QX, respectively.

in section 3.2.2, PZ was always excited at 365 nm ($\pi\pi^*$ transition, $S_3 \leftarrow S_0$), where the absorbing transition dipole is polarized in the long x axis of the molecule. The phosphorescence was detected in the origin of the spectrum at 638 nm where the phosphorescence is strongly negatively polarized [$P \equiv (I_{\parallel} - I_{\perp})/(I_{\parallel} + I_{\perp}) = -0.27$, see Figure 2].

Quinoxaline. From the phosphorescence decay of QX in 3MP on a millisecond scale, a total triplet lifetime $\tau_{0,qx} = 1/k_{0,qx} = 265.2 \pm 0.2$ ms was found, which agrees well with the average lifetime $\langle k_i \rangle^{-1} = 248.1$ ms, calculated with the values for k_i given in Table 1. QX was excited at 308 nm ($\pi\pi^*$ transition, $S_2 \leftarrow S_0$), where the absorbing transition dipole is polarized in the molecular plane of the molecule. The phosphorescence was detected in the second vibronic band of the spectrum at 500 nm, where the phosphorescence is strongly negatively polarized ($P = -0.23$, see Figure 2).[26]

3.2. Spin-Lattice Relaxation. Substate-specific properties of the triplet state of either compound are listed in Table 1. According to different magnetic resonance experiments on molecular crystals,[4,17,27,28] the initially most populated triplet substate (T_{1x}, probability of population by selective ISC > 95%) is also the most phosphorescent one (cf. Table 1). Because in thermal equilibrium at temperatures T > 70 K the population of the three triplet substates is nearly equal, the phosphorescence intensity must drop to ≈1/3 of its initial value after laser excitation. Due to this fact, it is possible to observe SLR without saturating one of the $T_{1i} \rightsquigarrow T_{1j}$ transitions (for further details see ref 2).

Figure 3 shows an example of the effect of SLR on the initial phosphorescence decay of PZ in 3MP at 75 K. To measure the initial decay of the phosphorescence after pulsed excitation, the emission intensity was monitored with a time resolution of 1 μs. Immediately after laser excitation (t = 0 can be found through back extrapolation, see the dotted line in Figure 3), the phosphorescence intensity drops, as expected, to ≈1/3 of its initial value. For the determination of SLR rates, I_{mag} was always

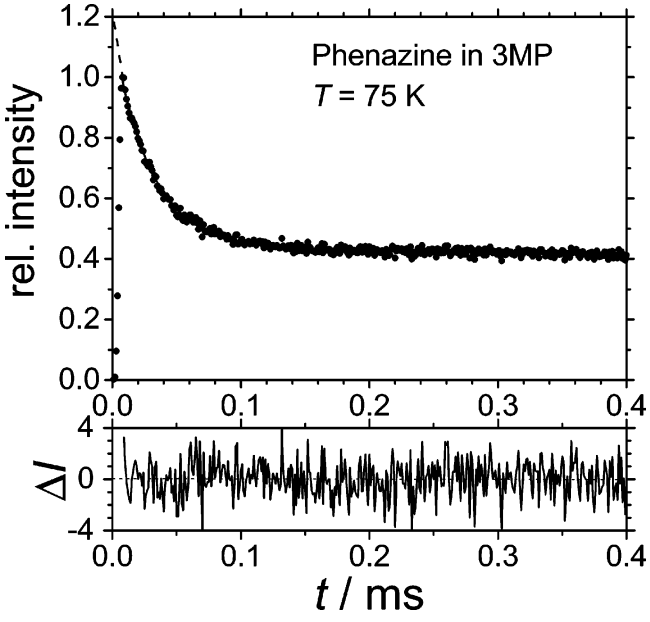

Figure 3. Effect of SLR on the phosphorescence of PZ in 3MP at 75 K. The phosphorescence decay, $I(t)$, was measured for $\kappa \approx 54.7°$ and described by eq 5. The dotted line is an extrapolation of the fit to the time of excitation. The channel dwell time was 1 μs. The lower part of the figure shows the weighted residuals of the fit: $\Delta I = (I_{exp} - I_{calc})/\sqrt{I_{exp}}$.

measured to eliminate the effect of OR. At temperatures where the viscosity of the solvent is sufficiently high (like in the example in Figure 3), OR plays no role for $I(t)$ because it is too slow to be observed, that is, $k_0 > k_r$. MER was eliminated for the measurement of SLR by using a broad-band interference filter for the measurement [$m(\lambda) \approx 0$ in eq 4]. Hence, eq 1 reduces to $I(t) = I_0 \exp(-k_0 t)\, f_s(t)$. In practice we used the following equation for the description of the time dependence of the phosphorescence intensity:

$$I(t) = U_s \exp(-k_0 t) + V_s \exp[-(k_s + k_0)t] \qquad (5)$$

where the ratio of the pre-exponential factors, $s = V_s/U_s$, depends on p_{i0} and $k_{i,rad}$ (see ref 2)

$$s = [(\Sigma_i^3 p_{i0} k_{i,rad})/(\Sigma_i^3 p_{i\infty} k_{i,rad})] - 1 \qquad (6)$$

The factor s, which theoretically can take a maximum value of s = 2, is a measure for OSP and will be discussed in section 3.2.2.

3.2.1. Dependence of SLR on Temperature and Viscosity. During the course of this investigation it was discovered that eq 5 is only valid in the high-temperature regime of SLR, which is essentially within and above the glass-transition range of the respective solvent. At lower temperatures where the alkane solvents form hard glasses, a third exponential is essential to describe the effect of SLR on the phosphorescence decay [rate coefficients k_0, k_{s1}, and k_{s2}; compare Figure 3 (T = 75 K) in this paper with the measurement at T = 40 K in part 2].[14] The temperature T_s at which it is possible to distinguish between one and two exponentials for SLR depends on the solvent. The accuracy with which T_s can be determined (±2 K in this study) depends on the time resolution of the measurement. In this paper we only report on the results of SLR for $T \geq T_s$, which we refer to as SLR_h,[2] whereas SLR below T_s, denoted as SLR_l, is discussed in detail in part 2.[14]

Figure 4 shows the temperature dependences of the rate constants k_s of PZ in four different alkane solvents and of QX

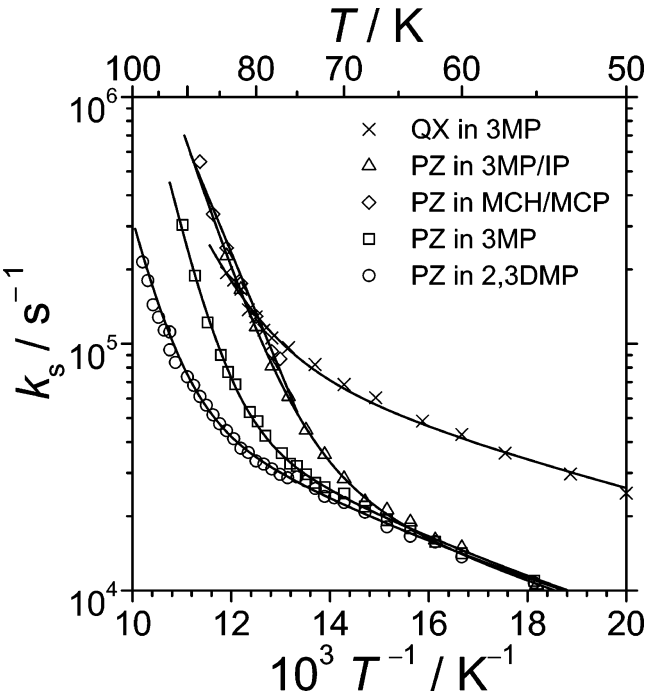

Figure 4. Temperature dependence of the effective rate coefficient k_s for PZ in 3MP, 3MP/IP, 2,3DMP, and MCH/MCP, as well as for QX in 3MP. The solid lines were calculated with eq 7. Parameter values are listed in Table 2.

TABLE 2: Parameter Values of Fits of Equation 7 to k_s as a Function of Temperature in the Glass-Transition Range of Several Solvents[a]

compound	solvent	A_s (s^{-1})	E_s (kJ mol^{-1})	B_s ($K^{-\alpha}$ s^{-1})	α
PZ	3MP	9.12×10^{14}	16.67	0.044	3.10
PZ	2,3DMP	1.61×10^{13}	15.10	0.089	2.92
PZ	3MP/IP	4.66×10^{12}	11.88	0.051	3.06
PZ	MCH/MCP	1.48×10^{11}	9.25		
QX	3MP	2.55×10^{11}	10.33	1.374	2.52

[a] See Figure 4.

in 3MP. On the basis of Figure 4, the distinction of two different mechanisms, SLR_h and SLR_l, becomes obvious. For PZ below 65 K, the solvent matrix becomes sufficiently rigid so that phonon processes, which are characteristic for a hard glass, dominate the spin relaxation. Within the glass-transition range, however, the different mobilities of the molecules in viscous solution gain influence on the spin relaxation. At temperatures $T > 65$ K, where SLR_h is dependent upon the respective solvent, we conclude that fast irreversible small-scale reorientations of the solute molecule as a result of rotational-diffusion processes lead to SLR_h. A structural relaxation process causing SLR_h is also strongly supported by the fact that the viscosities of the solvents, η(2,3DMP) > η(3MP) > η(3MP/IP), show the same relation as the respective relaxation times for SLR_h, τ_s(2,3DMP) > τ_s(3MP) > τ_s(3MP/IP); they are compatible. The SLR_h mechanism is, hence, expected to be thermally activated over small enough temperature ranges. We found that k_s as a function of temperature can be sufficiently well-described by

$$k_s(T) = A_s \exp(-E_s/RT) + B_s T^{\alpha} \qquad (7)$$

over the temperature range shown in Figure 4. The solid line in Figure 4 was calculated by means of eq 7; parameter values are given in Table 2.

The first term in eq 7 accounts for a thermally activated process due to rotational diffusion, where A_s is a fitting parameter and E_s is the associated activation energy. The second term in eq 7 accounts essentially for properties of the solid solution in the glass transition. Freezing a glass-forming liquid leads, according to the "model of the free volume", to islands of mobility and nonmobility, which possess properties of viscous liquids as well as vitreous solids.[29] The fitting parameter α in eq 7 yielded the value of 3 for all solvents and characterizes the temperature dependence of phonon processes active in the glass.[14] In the glass-transition range, the second term contributes only up to 1/6 of the total value of k_s.

TABLE 3: SLR Times, $\tau_s = 1/k_s$, from a Fit of Equation 5 to the Phosphorescence Decays of PZ in 2,3DMP at Temperatures between 68 and 98 K[a]

T (K)	τ_s (μs)	$s = V_s/U_s$	T (K)	τ_s (μs)	$s = V_s/U_s$	T (K)	τ_s (μs)	$s = V_s/U_s$
68.0	48.14	1.70	79.0	30.71	1.76	89.0	14.73	1.68
70.0	43.89	1.71	80.0	29.83	1.71	90.0	13.61	1.64
71.0	42.06	1.70	81.0	27.55	1.66	91.0	11.90	1.66
72.0	41.53	1.46	82.0	26.53	1.71	92.0	10.59	1.65
73.0	38.63	1.65	83.0	24.25	1.70	93.0	8.94	1.73
74.0	36.00	1.59	84.0	22.50	1.71	94.0	8.81	1.43
75.0	34.66	1.53	85.0	21.11	1.70	95.0	7.81	1.42
76.1	34.89	1.81	86.0	19.42	1.72	96.0	6.94	1.34
77.0	33.84	1.78	87.0	17.75	1.70	97.0	5.54	1.33
78.0	32.13	1.79	88.0	16.35	1.67	98.0	4.66	1.50

[a] Values of the ratio of pre-exponential factors in eq 5 are also given.

The activation energies, E_s, in Table 2 are similar to values reported by Gillies et al.[30] who also found Arrhenius behavior of SLR in benzile crystals at temperatures between 130−217 K with activation energies of ≈13 kJ mol^{-1}. The remarkably good agreement with activation energies in Table 2 may be accidental for two reasons: (A) The benzile crystal in ref 30 is a rigid host matrix and not a highly viscous solution. (B) In undoped crystals, effects based on triplet excitons cannot be ruled out. In molecular crystals, defects or impurities can influence SLR through (X−) trapping or thermally activated detrapping of the exciton energy.

3.2.2. Dependence of SLR and OSP on the Excitation Wavelength. The factor $s = V_s/U_s$ from eq 5 was calculated for all measurements, and it was found that, to a good approximation, it is independent of the temperature (see Table 3). Therefore, we calculated the average value, $\langle s \rangle$, for all temperatures in the glass-transition range for each solvent. The following values were found for PZ: $\langle s \rangle = 1.70$ in 3MP, $\langle s \rangle = 1.65$ in 2,3DMP, $\langle s \rangle = 1.46$ in 3MP/IP, and $\langle s \rangle = 1.23$ in MCH/MCP. For QX in 3MP, $\langle s \rangle = 1.68$ was calculated. The accuracy of $\langle s \rangle$ is better than 10% in all cases. The error associated with s is due to the uncertainties of the amplitudes U_s and V_s, which are based on the back extrapolation of t to the time of excitation ($t = 0$). Because the time resolution of the measurement is limited (1 μs) for decreasing SLR times, at high temperature, s values become less accurate. Because only measurements at high temperatures were performed in MCH/MCP, this may explain the particularly small value for $\langle s \rangle$ for this solvent. Values for s and SLR times, $\tau_s = 1/k_s$, listed in Table 3, are exemplary for measurements of PZ in 2,3DMP between 68 and 98 K.

With the known literature values for p_{i0} and $k_{i,rad}$ in Table 1,[4,27] s was also estimated using eq 6. Values of $s = 1.78$ and $s = 1.77$ were found for PZ and QX, respectively. These results, which are associated with measurements at $T < 2$ K,[4,27] agree reasonably well with our values of $\langle s \rangle$. All averages are, however, systematically somewhat smaller than 1.77, especially for the solvent mixtures. This indicates that OSP in organic glasses does not lead to such extreme ratios of the initial

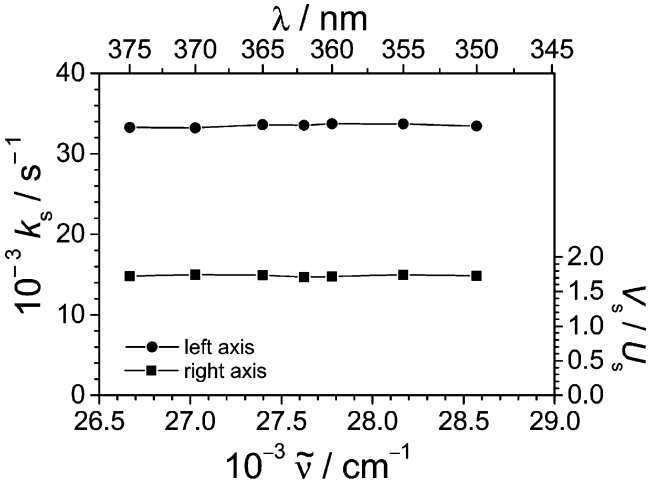

Figure 5. Effective rate constants k_s and ratios $s = V_s/U_s$ for PZ in 2,3DMP at 80 K as a function of the excitation wavenumber. For the shown measurements, $k_s = (33.4 \pm 0.2) \times 10^3$ s^{-1} and $s = 1.73 \pm 0.01$.

populations of the triplet substates, p_{i0} ($i = x, y, z$; Table 1), as in molecular crystals at low temperatures.

OSP is expected to be independent of the excitation wavelength if the lifetime τ_1 of S_1 is substantially longer than the averaged relaxation time τ_{vr} of nuclear vibrations. This is definitely not the case for PZ. Because for PZ $\tau_1 \sim \tau_{vr}$ in S_1, ISC must predominantly occur from vibrationally excited states (*) if the molecules are not excited in the 0,0 transition of the $S_1 \leftarrow S_0$ absorption band: $S_1^* \rightsquigarrow T_n^* \rightsquigarrow T_1^* \rightsquigarrow T_1$. Because selection rules play an important role for OSP, we investigated whether OSP was dependent on the initially excited vibrational mode by measuring SLR times at different excitation wavelengths. We used the s values obtained as a measure for OSP. In Figure 5, the SLR rate coefficients k_s and the quotients s are shown as a function of the phosphorescence excitation wavelength. All measurements in this figure refer to PZ in 2,3DMP at 80 K. Figure 5 shows that OSP is virtually independent of the vibrational state from which ISC occurs because s and k_s are practically constant for excitation wavelengths covering a region of approximately 2000 cm^{-1}, where the S_2 and S_3 absorption bands overlap.

3.3. Orientational Relaxation. The effect of OR was studied by measuring the time-dependent phosphorescence intensity $I_{||}(t,\kappa = 0°)$ or $I_{\perp}(t,\kappa = 90°)$. The strongly negative polarization of the phosphorescence of PZ at 638 nm and QX at 500 nm (see Figure 2) leads to an initial increase or an initial decrease in the phosphorescence intensity when $I_{||}(t)$ or $I_{\perp}(t)$ are measured, respectively. An example of this phosphorescence-depolarization effect due to slow complete OR is shown in Figure 10 of ref 2. When OR was observed, the relation $k_s \gg k_e > k_r$ held. Therefore, SLR was entirely negligible and the time dependence of the phosphorescence was well-described by (cf. eqs 1 and 3)

$$I(t) = U_r \exp(-k_0 t) + V_r \exp[-(k_r + k_0)t] \qquad (8)$$

where $U_r = I_0$ and $V_r = I_0(1/5)[3\cos^2(\delta) - 1][3\cos^2(\kappa) - 1]$. The fact that k_e is only by a factor of $\approx$10 larger than k_r for a given temperature had to be considered at lower temperatures where the mean solvation time becomes long enough to be noticeable in the phosphorescence decay. Although an interference filter was used for the phosphorescence detection to minimize the solvation effect on the emission intensity, up to the first 100 μs were omitted in fits of eq 8 to the time-dependent phosphorescence to avoid any distortions of the analysis results. From the fits, k_r and k_0 were determined; values found for k_0 were in satisfactory agreement with the results presented in section 3.1.

One can derive the mean value $\langle\delta\rangle$ for the angle between the dipole moments of absorption and emission from the intensities $I_{||}(t = 0)$ and $I_{\perp}(t = 0)$, which are obtained by extrapolation of the phosphorescence decay to the time $t = 0$. For PZ in 3MP, averaging over results at all temperatures yields $\langle\delta\rangle = 77.6 \pm 10.0°$, which corresponds to a polarization degree of $P(0) = P_2(\cos\delta)[\cos 2(\delta) + 3]^{-1} = -0.28 \pm 0.05$.[31,32] For QX in 3MP, $\langle\delta\rangle = 72.5 \pm 8.0°$, which corresponds to $P(0) = -0.23 \pm 0.07$. This is in excellent agreement with the measurement of the polarization degree shown in Figure 2. The theoretical minimum of $P = -1/3$ (see ref 32) is obviously not reached for either compound (see Figure 2). Two different interpretations of this result are conceivable:

(1) Besides slow complete reorientation of solute molecules as a result of rotational diffusion, OR is also expected to possess faster components of a librational nature. One way to account for faster components of OR is to use an ansatz of $\rho(t) = \Sigma_j c_j \rho_j(t)$ in eq 3 with $\rho_j(0) = 1$, $\rho_j(\infty) = 0$, and $\Sigma_j c_j = 1$. If each component ρ_j can be represented by a single exponential, $\exp(-k_j t)$, then obviously only the slowest component of OR is probed in our experiments. Fast reorientational motions remain unobserved; they contribute, however, to the depolarization of the phosphorescence. This may explain why even in strongly negatively polarized transitions, $P = -1/3$ is generally never reached. The angle $90° - \langle\delta\rangle$ would then become a measure for the contribution of the fast unobservable components of OR to the overall depolarization. These components may even be active in solid solutions as a result of their librational character. Solvation dynamics might conceivably account for such a fast component (cp. section 3.5).

(2) If $\langle\delta\rangle < 90°$ is caused by the fact that two differently polarized transitions of the phosphorescence are superimposed, then $\langle\delta\rangle$ would not have a simple physical meaning. In that case, $\langle\delta\rangle$ would be strongly dependent upon the excitation and detection wavelength and, therefore, would only have formal character. Only by detecting at a wavelength at which the polarization degree is $P \approx 0$ (for PZ at 660 nm for instance, see Figure 2), one could predict an average angle between the transition dipoles of $\langle\delta\rangle \approx 54.7°$ (magic angle).[22] Experiments to test this interpretation were, however, not performed.

3.3.1. Dependence of OR on Temperature and Viscosity. The measurements of OR times, $\tau_r = 1/k_r$, were limited at low temperatures by the triplet lifetimes of PZ and QX and at high temperatures by the time resolution of the experimental setup. Because QX has a much longer triplet lifetime than PZ, OR times for QX are by a factor of 20 longer in the present work than for PZ at the lowest temperatures. The OR rate coefficients $k_{r||}$ and $k_{r\perp}$, which were obtained by fitting eq 8 to $I_{||}(t)$ and $I_{\perp}(t)$, agree rather well. This is demonstrated in Figure 6, where $k_{r||}$ and $k_{r\perp}$ are displayed as a function of the reciprocal temperature.

The temperature dependence of k_r, which was calculated as the average $^1/_2(k_{r||} + k_{r\perp})$, was satisfactorily described by an Arrhenius law

$$k_r(T) = A_{r,Arr} \exp[-E_{r,Arr}/(RT)] \qquad (9)$$

The corresponding values of the temperature-independent activation energies $E_{r,Arr}$ and the parameters $A_{r,Arr}$ are shown in Table 4. The extremely large frequency factors $A_{r,Arr}$ in Table 4 indicate, however, that the description of OR rates by an

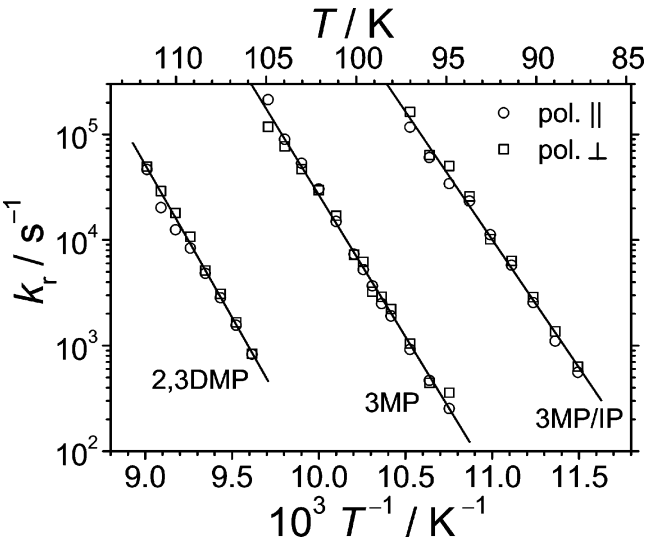

Figure 6. Arrhenius plot of the rate constants k_r for PZ in the solvents 2,3DMP, 3MP, and 3MP/IP. Circles and squares refer to different polarization directions. The solid lines were calculated with eq 9, and the corresponding parameters are listed in Table 4.

TABLE 4: Parameter Values of Equations 9 and 10[a,b]

compound	solvent	eq	A_r (s^{-1})	E_r (kJ mol^{-1})	T_0 (K)
PZ	3MP	9, Arr	2.09×10^{31}	51.48	
PZ	3MP	10, VFT	4.43×10^{16}	11.10	52.5
PZ	2,3DMP	9, Arr	5.13×10^{30}	55.30	
PZ	2,3DMP	10, VFT	1.01×10^{18}	15.40	50.7
PZ	3MP/IP	9, Arr	4.82×10^{30}	46.43	
PZ	3MP/IP	10, VFT	1.48×10^{14}	6.78	56.0
QX	3MP	9, Arr	1.32×10^{33}	52.00	
QX	3MP	10, VFT	5.49×10^{16}	11.47	49.6

[a] Equations 9 and 10 were fitted to $k_r = {}^1/_2(k_{r\parallel} + k_{r\perp})$ as a function of temperature. [b] The detection wavelength was either 636 or 640 nm for PZ and 500 nm for QX.

Arrhenius law is not necessarily meaningful. The Arrhenius fit, hence, has empirical character and is likely to yield satisfactory values only over the temperature range shown; extrapolations may only be adequate up to temperatures where the increase of T/η (η = viscosity of the solvent) is not larger than a factor of $\approx$10. The introduction of a temperature-dependent activation energy, $E_{r,VFT}(T) = E_{r,Arr}[T/(T - T_0)]$, drastically reduces the pre-exponential factor. Fits of the Vogel−Fulcher−Tammann (VFT) law,[33]

$$k_r(T) = A_{r,VFT} \exp[-E_{r,VFT}/R(T - T_0)] \qquad (10)$$

to k_r values as a function of T^{-1} are shown in Figure 7 (dashed lines) for all measurements; parameters are also listed in Table 4. The temperature T_0 in eq 10 is like the glass-transition temperature T_g, a characteristic quantity for a glass-forming liquid,[34] and is generally between 20 and 40 K lower than T_g.[35,36] All values for T_0 agree surprisingly well (within 10%) with values that were found in the description of the temperature dependence of the solvents' viscosities, $\eta(T)$, by a VFT law in the highly viscous regime.[11,36]

For measurements of PZ in different solvents, it is expected that OR times increase with increasing solvent viscosity, that is, with increasing molecular friction. This is evident in Figure 7. By comparing OR times of PZ in 3MP with those of QX in 3MP, one may qualitatively expect τ_r(PZ) to be similar or somewhat larger than τ_r(QX) because QX is only slightly smaller than PZ ($D_{\perp,QX} > D_{\perp,PZ}$) and, therefore, assumingly less solvent molecules of the solvent cage take part in rotations over

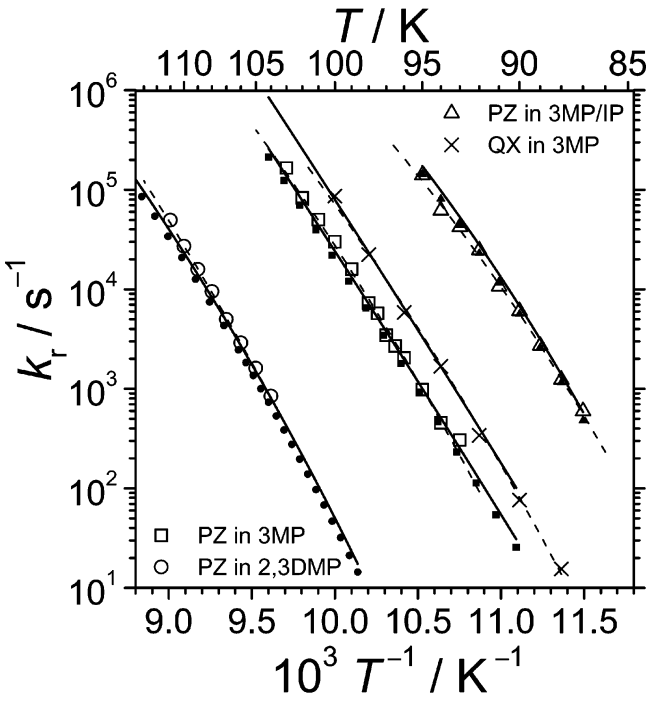

Figure 7. Temperature dependence of the mean rate constants $k_r = {}^1/_2(k_{r\parallel} + k_{r\perp})$ (big hollow symbols) for PZ in the solvents 2,3DMP, 3MP, and 3MP/IP, as well as for QX in 3MP. The dashed lines were calculated with eq 10, and the corresponding parameter values are listed in Table 4. The smaller symbols are calculated with eqs 11−13 for $q = a/b = a/c = 2$ (also see text). The solid lines were calculated with eq 14 for an asymmetric ellipsoid in the limit of slip boundary conditions. Values for D_i (i = 1, ..., 3) were calculated using $\kappa_1 = 0.07$, $\kappa_2 = 7.85$, and $\kappa_3 = 7.08$ for PZ (ellipsoid: $a/b = 0.33$ and $a/c = 0.3$) and $\kappa_1 = 1.58$, $\kappa_2 = 6.21$, and $\kappa_3 = 1.58$ for QX (ellipsoid: $a/b = 0.6$ and $a/c = 0.3$).[44]

reasonably large angles. Thus, the mechanical friction with the solvent is expectedly lower for QX and rotational-diffusion processes are less hindered than for PZ. If dielectric friction played a role at all in a non-dipolar solvent such as 3MP, the interaction of QX with the solvent molecules would even increase the OR times of QX compared to those of PZ as a result of their difference in dipole moment. To our surprise, however, the mean difference between the OR times of PZ and the OR times of QX turned out to be rather large: $k_r(QX) \approx 3k_r(PZ)$ (see Figure 7). This large difference must be mainly based on the different dimensions of the molecules. Because a single exponential was sufficient to describe the time-dependent phosphorescence depolarization, we used the modified Debye−Einstein equation,[18,20,37]

$$\tau_r = (6D_\perp)^{-1} = (V_m \eta C)/[\Phi(q) k_B T] \qquad (11)$$

to calculate absolute values of τ_r. In a first approach, we applied eq 11 assuming (*i*) "stick" boundary conditions,[38] that is, $C = 1$, and (ii) that the rotating molecule can be approximated by a symmetrical rotational ellipsoid[39] with a long half axis, a, and short rotational half axes, b and c (with $b = c$). Because the transition dipole moment is quantized along the long axis for PZ[40] and QX[41] at the respective excitation wavelengths (x axis in Figure 1), both molecules were approximated by a prolate ellipsoid ($a > b$). In eq 11, $D_\perp$ is the rotational-diffusion coefficient for rotations about one of the short axes, V_m is the effective molecular volume, η is the solvent's viscosity, and $\Phi(q)$ is a form factor that depends on the ratio $q = a/b$. $\Phi(q)$ is given by[18]

$$\Phi(q) = \frac{3q[(2q^2-1)Y - q]}{2(q^4-1)} \tag{12}$$

where the quantity Y depends on the sign of $q - 1$. For $q > 1$ (prolate ellipsoid) Y is given by[18]

$$Y = \frac{\ln[q + \sqrt{(q^2-1)}]}{\sqrt{(q^2-1)}} \tag{13}$$

The effective volume V_m is obtained from the density ρ and the molar mass M of crystalline PZ and QX at room temperature, $V_m = FM(\rho N_a)^{-1}$, assuming a space-filling factor $F \approx 0.8$. Using $\rho \approx 1.34$ g cm^{-3} and $M = 180.21$ g mol^{-1} for PZ yields $V_{m,PZ} \approx 1.7 \times 10^{-22}$ cm^3, and for QX, $V_{m,QX} \approx 1.4 \times 10^{-22}$ cm^3 is estimated using $\rho \approx 1.13$ g cm^{-3} and $M = 130.15$ g mol^{-1}. The viscosities, $\eta(T)$, which cover the relevant temperature ranges for 3MP and 2,3DMP, were taken from VFT fits in ref 11, where new data were taken with a falling-ball viscosimeter. For measurements in 3MP/IP, values of η below 90 K are extrapolated and are taken from Ruth et al.[36] With a ratio of $q = 2$ [i.e., $\Phi(2) = 0.6645$] for PZ, adequate values for the OR rates were obtained for measurements in 3MP/IP, as shown by the small solid symbols in Figure 7. For PZ in 3MP, values of k_r appear to be somewhat too small, and in 2,3DMP, k_r is even systematically too small for all temperatures. This indicates a significant deviation from the "stick" boundary condition for the corresponding solvent−solute combinations. Using a reasonable ratio of $q = 1.3$ [i.e., $\Phi(1.3) = 0.9112$] for QX yielded values for k_r that are a factor of ≈2.4 smaller than the measured values (not shown in Figure 7). This means that an empirically determined factor $C \approx 0.42$ in eq 11 would produce much better OR rates in the case of QX, which corroborates a severe flaw of the assumption of "stick" boundary conditions in the present case. An attempt to approximate QX by an oblate symmetrical ellipsoid on the basis of the assumption that a significant component of the transition dipole moment is quantized along the short in-plane axis (a superposition of transition moments is possible in the inhomogeneously broadened absorption band)[41] also yielded even smaller orientational rate coefficients for "stick" boundary conditions.

To address the shortcomings of the above considerations, the factor $\zeta = 6V_m\eta C\Phi^{-1}$, which represents the hydrodynamic rotational friction coefficient, was calculated for "slip" boundary conditions,[42] assuming an asymmetric rotational ellipsoid. Because the transition dipole moment is oriented along the long axis for PZ and QX, and since only a single exponential was observed in the time-dependent phosphorescence depolarization, the OR times were calculated using[43]

$$\tau_r = \frac{1}{12}\left(\frac{4D_1 + D_2 + D_3}{D_1D_2 + D_2D_3 + D_3D_1}\right) \tag{14}$$

where $D_i = k_BT/(V_m\eta\kappa_i)$ are the diffusion coefficients along the long axis (x; $i = 1$), the short in-plane axis (y; $i = 2$), and the out-of-plane axis (z; $i = 3$). Values for κ_i are listed for a general ellipsoid in ref 44; for PZ we used interpolated values. The solid lines in Figure 7 correspond to the best results of OR rates calculated with eq 14 using $\kappa_1 = 0.07$, $\kappa_2 = 7.85$, and $\kappa_3 = 7.08$ for PZ [ellipsoid: $b/a = 0.33$ ($= q^{-1}$) and $c/a = 0.3$] and $\kappa_1 = 1.58$, $\kappa_2 = 6.21$, and $\kappa_3 = 1.58$ for QX [ellipsoid: $b/a = 0.6$ ($= q^{-1}$) and $c/a = 0.3$].[44] The ellipsoidal dimensions for the two molecules are quite different in comparison to the previous approach where, on the basis of geometrical considerations, the ratios $q^{-1} = 0.5$ and $q^{-1} = 0.75$ were assumed for PZ and QX, respectively. OR rates for PZ in different solvents are equally well-described by the same asymmetric ellipsoidal geometry (see Figure 7). This corroborates the validity of "slip" boundary conditions, which should not vary for very similar nonpolar solvents made up of molecules that are smaller than the solute. The model only comprises the hydrodynamic friction of a continuum fluid; the contribution of dielectric components to the friction coefficient cannot easily be quantified and should, in the present context, be of negligible relevance.

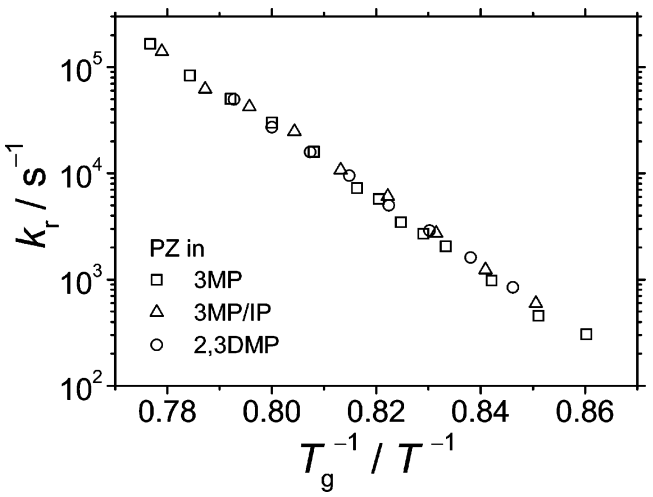

Figure 8. Master plot of OR rates. The rates k_r were scaled according to the glass-transition temperatures, T_g(2,3DMP) ≈ 88 K, T_g(3MP) ≈ 80 K, and T_g(3MP/IP) ≈ 74 K.[36]

Our results concerning OR rates of QX in 3MP are in agreement with recently published data by Yang and Richert[45] who measured OR rates at lower temperatures between ≈82 and 88 K, whereas we covered the range from 88 to 100 K. At first glance, their value of $k_r \approx 200$ s^{-1} at 88 K (from Figure 5 in ref 45) seems to disagree with ours, k_r(88 K) ≈ 15.5 s^{-1}. This discrepancy is, however, due to the fact that the recorded temperature of the liquid in ref 45 was possibly 2−3 K lower than the actual temperature, as stated in the corresponding experimental section.[45] Because we find a VFT-interpolated value of $k_r = 200$ s^{-1} at ≈91 K, which is 3 K above the temperature shown in ref 45, the two measurements are in agreement. Moreover, Yang and Richert also report single exponential behavior of the time-dependent anisotropy, and they also found the temperature dependence to be satisfactorily described by a VFT law, in agreement with our data.

3.3.2. Scaling of OR in Different Solvents. An empirical relation between the rate coefficients of OR in different solvents follows from the concept of corresponding states[46] which relates different quantities of molecular relaxation phenomena by a simple scaling law. In the present case, a temperature scaling using a single factor, g_r, connects the temperature dependences of OR rate coefficients for different alkane solvents in the following way:

$$k_r^{3MP}(T) \approx k_r^{3MP/IP}(g_{r1}T) \tag{15a}$$

$$k_r^{3MP}(T) \approx k_r^{2,3DMP}(g_{r2}T) \tag{15b}$$

with $g_{r1} \approx 1.081$ and $g_{r2} \approx 1.189$. The factors g_r correspond to the ratio of the respective glass-transition temperatures[36] of the different solvents. If one normalizes the reciprocal temperature scales in Figure 7 for the different sets of OR measurements in 3MP, 3MP/IP, and 2,3DMP to the glass temperature T_g^{-1} of

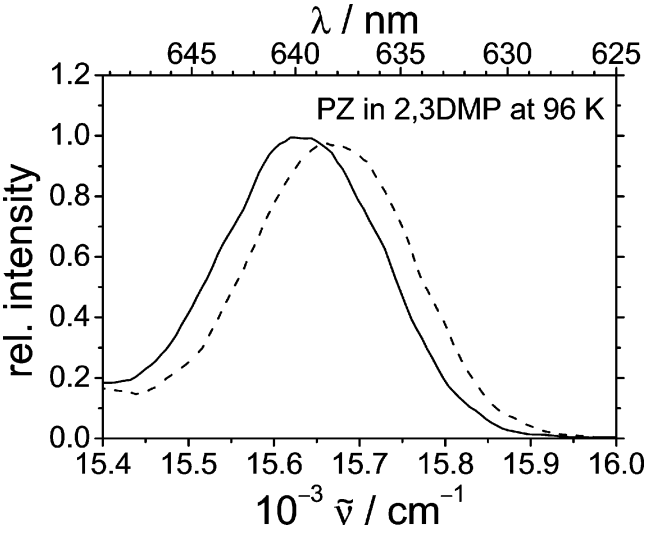

Figure 9. Time-dependent red shift of the 0,0 transition of the phosphorescence of PZ in 2,3DMP at 99 K. Dashed line: delay after excitation 5 μs, gate width 20 μs. Solid line: delay 20 ms, width 0.5 ms. Total shift $\approx$ 24 cm^{-1}.

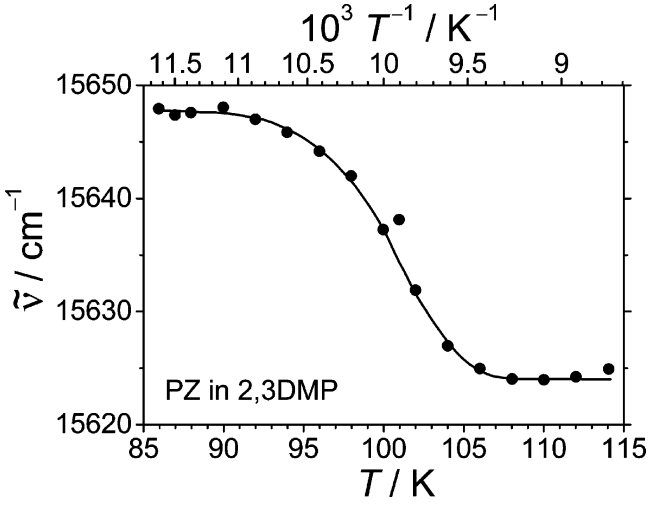

Figure 10. Temperature dependence of the center wavenumber of the 0,0 band of the phosphorescence of PZ in 2,3DMP measured 25−75 μs after excitation. $\tilde{\nu}(0) = 15\,648$ cm^{-1} and $\tilde{\nu}(\infty) = 15\,624$ cm^{-1} used in eq 16 are taken from this graph.

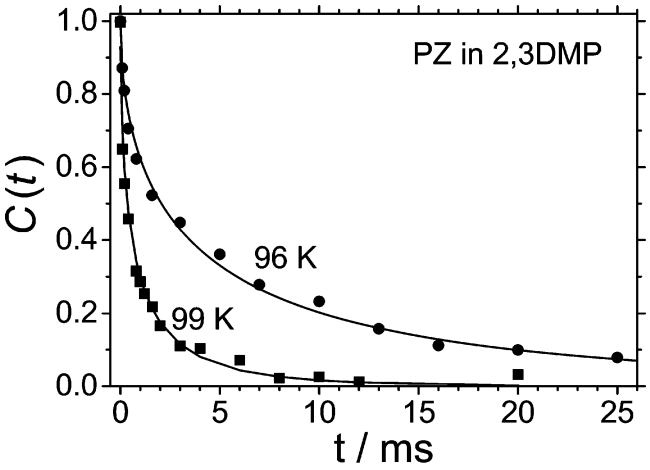

Figure 11. Stokes shift correlation function of PZ in 2,3DMP at 96 K (●) and 99 K (■) according to eq 16. The time window per data point increases with increasing time. The solid lines were calculated with eq 17 using the parameters $\tau_{kww}(96\text{ K}) = 4.1 \pm 0.5$ ms and $\tau_{kww}(96\text{ K}) = 0.70 \pm 0.04$ ms. $\beta_{kww} = 0.53 \pm 0.08$ in both cases.

one of the solvents (e.g., 3MP), the data will produce a single universal curve (master plot), see Figure 8.[47] This shows that the concept of corresponding states is applicable in the present case. It has the advantage that only one parameter, g_r, is necessary to correlate two different sets of relaxation measurements. For the scaling in Figure 9, glass-transition temperatures of T_g(3MP) $\approx$ 80 K, T_g(3MP/IP) $\approx$ 74 K, and T_g(2,3DMP) $\approx$ 88 K were used.[36] The latter value is somewhat higher than T_g(2,3DMP) $\approx$ 85 K, estimated in ref 36. The glass-transition temperatures of 2,3DMP and 3MP are in sufficient agreement with the values of T_g(2,3DMP) $\approx$ 87.5 K and T_g(3MP) $\approx$ 78.5 K stated in ref 48.

A bifurcation of the OR process, which was predicted by us[2] to occur in the temperature range investigated, could *not* be confirmed. The reasoning in ref 2 was based on the discrepancy between calculated and measured relaxation times, τ_r, at low temperature. The fact that in total only a few data points were available at the time of publication of ref 2 increased the significance of each measurement, and, therefore, results were overinterpreted.

3.4. MER (Solvation)—Temperature Dependence. The solvation of triplet-state molecules, which only requires the partial reorientation of solute and solvent molecules, can be observed in highly viscous solution through a time-dependent red shift of the phosphorescence. Figure 9 shows the 0,0 band of the phosphorescence spectrum of PZ in 2,3DMP at 99 K in two time windows after excitation: 5−20 μs and 20.0−20.5 ms. The total red shift of the spectrum of $\approx$24 cm^{-1} is small due to the fact that PZ has no permanent dipole moment and 2,3DMP is also a non-dipolar solvent. In polar liquids, red shifts of several hundred wavenumbers have been reported.[49−51] The dynamics of the solvation process can be studied by measuring the position of the 0,0 band as a function of time.[12,23] The same part of the spectrum, up to the onset of the first vibronic contour band, was always measured for this purpose. The spectral position of the band was determined through the mean wavenumber, $\tilde{\nu}(t)$, which is the point in the spectrum that halves the area under the band. The time-dependence of the red shift was described by the Stokes shift correlation function,[12,51,52]

$$C(t) = \frac{\tilde{\nu}(t) - \tilde{\nu}(\infty)}{\tilde{\nu}(0) - \tilde{\nu}(\infty)} \qquad (16)$$

which is normalized to the time of excitation, that is, $C(0) = 1$ and $C(\infty) = 0$. In eq 16, $\tilde{\nu}(0)$ and $\tilde{\nu}(\infty)$ are the limiting values of the mean wavenumber at the time of excitation and after fully completed solvation, respectively. $\tilde{\nu}(0)$ and $\tilde{\nu}(\infty)$ can be determined from the temperature dependence of the Stokes shift, as illustrated in Figure 10, where the mean wavenumber in the time window between 25 and 75 μs after excitation is shown as a function of temperature for PZ in 2,3DMP. Figure 10 shows that, in the vicinity of the glass-transition temperature ($T_g \approx 88$ K in 2,3DMP) and at higher temperatures (>104 K), the mean wavenumber appears to be largely temperature-independent. This is due to the fact that changes in the spectrum become too slow or too fast to be easily measurable, respectively. The values of $\tilde{\nu}(86\text{ K}) = 15\,648$ cm^{-1} and $\tilde{\nu}(114\text{ K}) = 15\,624$ cm^{-1} in Figure 10 were, therefore, associated with $\tilde{\nu}(0)$ and $\tilde{\nu}(\infty)$ in eq 16, assuming that $\tilde{\nu}(0)$ is indeed temperature-independent and that $\tilde{\nu}(\infty)$ is reached for all temperatures after a sufficiently long time.

An example of the correlation function $C(t)$ in eq 16 is shown in Figure 11 for PZ in 2,3DMP at 96 and at 99 K. The time window for each data point in Figure 11 increases with increasing time, and all measurements were taken in the linear-

response regime.[53] $C(t)$ generally exhibits nonexponential behavior in highly viscous glass-forming solvents[12,23] and can be described by the empirical Kohlrausch−Williams−Watts function

$$C(t) \propto \exp\left(-\frac{t}{\tau_{sol}}\right)^{\beta_{sol}} \quad (17)$$

The solid lines in Figure 11 were calculated with $\tau_{sol}(96\ K) = 4.1 \pm 0.5$ ms and $\tau_{sol}(99\ K) = 0.70 \pm 0.04$ ms. The same nonexponentiality parameter $\beta_{sol} = 0.53 \pm 0.08$ could be used for both correlation functions measured at 96 and 99 K. This is expected owing to the small difference in temperatures of only 3 K (compare with Table 1 in ref 45). A nonexponentiality parameter $\beta_{sol} = 0.5$ was also found in solvation studies of PZ in 2-methyltetrahydrofuran[54] and of QX in 2,3DMP (85−96 K) and in 3MP (74−88 K) by Yang and Richert.[45]

With increasing temperature, the initial shift of the spectrum after excitation becomes very fast (see, e.g., Figure 3 in ref 12). As a result of this critical temperature dependence of $C(t)$, the characteristic solvation time, τ_{sol}, can no longer be easily determined through fits of eq 17 to experimental data on the basis of the dynamic red shift of the spectrum.

However, because the solvation also affects the time-dependent phosphorescence as outlined in the introduction (cf. eq 4), the phosphorescence of PZ was systematically measured in the turning points of the 0,0 transition to establish the temperature-dependent behavior of solvation dynamics on the basis of this purely qualitative description.

For PZ, the phosphorescence was detected at 635 nm (short-wavelength side of the 0,0 band—"blue") and at 643 nm (long-wavelength side of the 0,0 band—"red") with a spectral resolution of 0.4 nm, using the magic angle to avoid any depolarization effects. At the temperatures where this simple approach was used, SLR is too fast to be observable with our time resolution. Figure 12 shows an example of the fast initial decrease or increase of the phosphorescence obtained upon photon detection in the "blue" and "red" edges of the 0,0 band, respectively. The maximum of the 0,0 band immediately after excitation is at ≈638 nm. Because in principle solvation is not complete even after times $t > \tau_0$, the normal triplet decay and the effect of solvation on the phosphorescence are not independent. In other words, boundary conditions to normalize the initial intensity change to the main triplet decay cannot be found in this approach. This is the reason for the effect being only qualitatively well-described by[55]

$$I_{mag}(t) = I_0 \exp(-k_0 t)\, f_e(\lambda,t) = U_e \exp(-k_0 t) + V_e \exp[-(k_e + k_0)t] \quad (18)$$

at temperatures where $k_e \gg k_0$. In eq 18, $U_e = I_0$ and $V_e = I_0 m(\lambda)$ (see eq 4). Rate coefficients, obtained upon detection on the "blue" ($k_{e,blue}$) and "red" ($k_{e,red}$) sides of the 0,0 band, were in good agreement and differed only by 3−25%. Hence, the overall rate coefficient was determined through $k_e = {}^1/_2(k_{e,blue} + k_{e,red})$.

The temperature dependence of k_e, which is only a *relative* measure for the time scale of solvation, is shown in Figure 13 for PZ in 2,3DMP, 3MP, and 3MP/IP and for QX in 3MP. At temperatures where k_e is not significantly larger than the triplet decay rate k_0, the factor $m(\lambda)$ becomes small and k_e apparently becomes temperature-independent. This is an artifact and illustrates at what temperature the empirical description of I_{mag} by eq 18 does not yield values of k_e anymore that are meaningful for the qualitative description of the temperature-dependent time

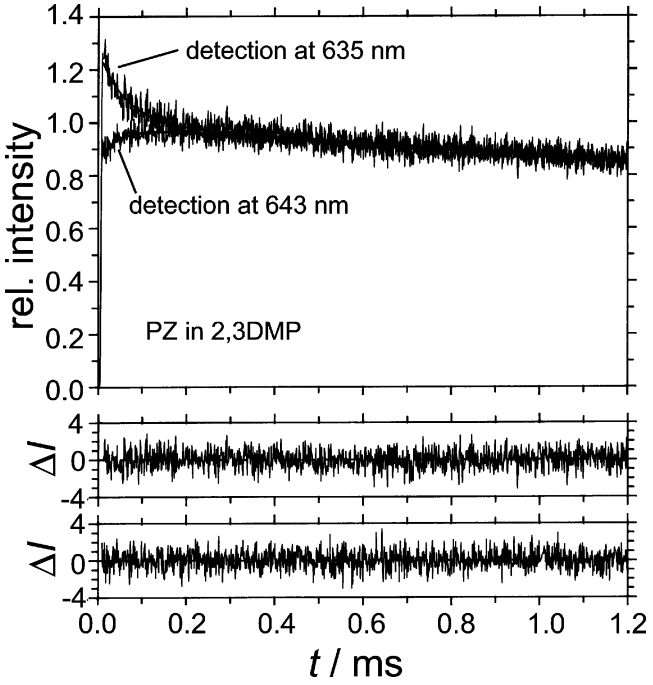

Figure 12. Phosphorescence decay (I_{mag}) of PZ in 2,3DMP at 104 K. The dynamic red shift of the spectrum leads to an initial increase or decrease of the phosphorescence, if the light is detected with a high spectral resolution (<0.4 nm) in the turning points of the 0,0 band, respectively (wavelengths shown in the graph). The lower part of the figure shows the weighted residuals of a fit of eq 18 to the experimental curve: $\Delta I = (I_{exp} - I_{calc})/\sqrt{I_{exp}}$.

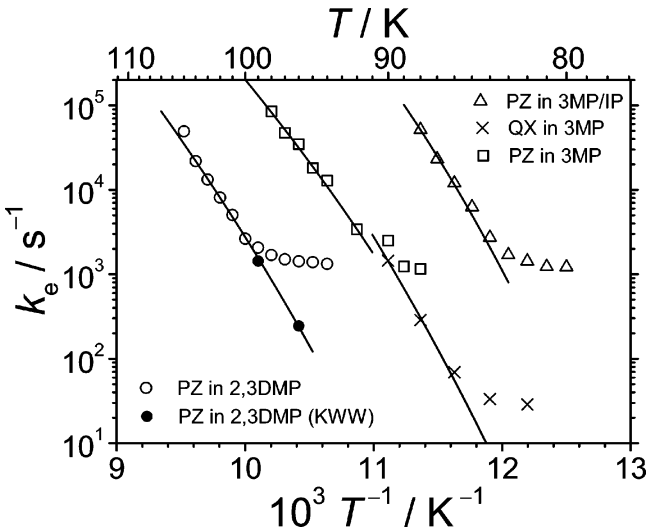

Figure 13. Activation plot of the averaged rate coefficients $k_e = {}^1/_2(k_{e,blue} + k_{e,red})$. The solid lines were calculated with eq 19; parameter values are listed in Table 5. The solid symbols correspond to the two measurements of $k_{sol} = 1/\tau_{sol}$ of PZ in 2,3DMP (see Figure 11).

scale of solvation. At higher temperatures, $k_e(T)$ can be represented by a VFT law:

$$k_e(T) = A_{e,VFT} \exp[-E_{e,VFT}/R(T - T_0)] \quad (19)$$

The solid lines in Figure 13 were calculated with eq 19, and the corresponding parameters are listed in Table 5. T_0 was taken from Table 4 and fixed for the fit of eq 19 to appropriate values of $k_e(T)$. The activation energies $E_{e,VFT}$ (Table 4) agree quite well with $E_{r,VFT}$ (Table 5), which means that the ratio k_e/k_r is not changing dramatically over the considered temperature range. This is in agreement with the results of Richert and co-

TABLE 5: Parameter Values of Equation 19[a,b]

compound	solvent	eq	A_e (s^{-1})	E_e (kJ mol^{-1})	T_0 (K)
PZ	3MP	19, VFT	1.11×10^{14}	7.95	52.5
PZ	2,3DMP	19, VFT	2.71×10^{15}	11.32	50.7
PZ	3MP/IP	19, VFT	2.97×10^{14}	5.98	56.0
QX	3MP	19, VFT	1.06×10^{16}	9.95	49.6

[a] Equation 19 was fitted to $k_e = {}^1/_2(k_{e,blue} + k_{e,red})$ as a function of temperature. [b] VFT parameter T_0 was fixed at the value found in the activation plot of OR rates. Compare with the values in Table 4.

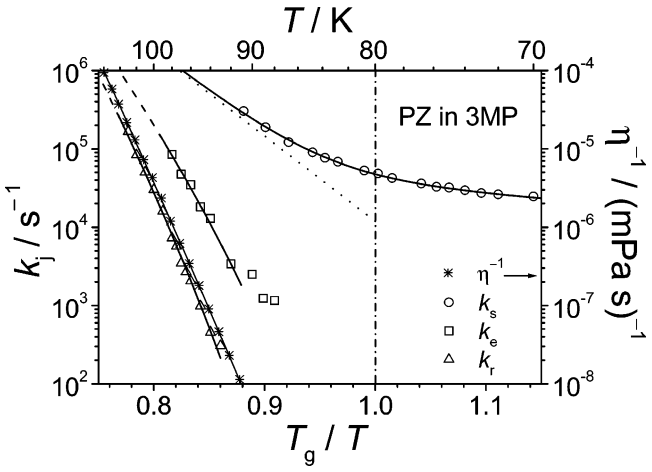

Figure 14. Comparison of the effective rate coefficients of OR (k_r), MER (k_e), and SLR (k_s) of PZ in 3MP (left axis), as well as the solvent's reciprocal viscosity, η^{-1} (right axis). The reciprocal temperature scale is normalized to T_g of 3MP at 80 K. The VFT description of OR and MER rates (solid lines) is extrapolated to higher temperatures (dashed lines). The description of SLR rates according to eq 7 (solid line) and their Arrhenius contribution (dotted line) above T_g are also shown. SLR below T_g will be discussed in part 2.[14]

workers[45,54] who reported OR times to be related to the characteristic solvation times by a temperature invariant factor for QX in various organic solvents. It is interesting to note that, for measurements of PZ in 2,3DMP, the two characteristic solvation rates $k_{sol} = 1/\tau_{sol}$ at 96 and 99 K (Figure 11) seem to agree quite well with the temperature-dependence of k_e (Figure 13). This good agreement on an absolute scale is probably accidental. It illustrates, however, that $k_e(T)$ seems to represent the relative change of solvation with temperature sufficiently well.

3.5 Relaxation Processes of SLR, OR, and MER (Solvation) in Comparison. In Figure 14, the effective rates of OR, MER, and SLR are semi-logarithmically shown (left axis) as a function of the reduced temperature (T_g/T) for PZ in 3MP. The inverse viscosity of the solvent is also shown (right axis) over the same number of decades as the rate coefficients. The experiments with the other solvents yielded qualitatively very similar graphs.[25] SLR is observable over the entire glass-transition range of the solvent. Structural changes of the matrix start to affect the SLR mechanism approximately in the vicinity of the glass-transition temperature, and some degrees below T_g, SLR cannot be characterized by a single rate coefficient, k_s, anymore. This aspect and the temperature dependence of SLR below T_g are the subject of part 2, ref 14. The number of data points above T_g is rather limited so that the description by an activated process, as shown by the dashed line in Figure 14, cannot be extrapolated far beyond the temperature range shown. In fact, the Arrhenius trace of SLR rates and the VFT trace of OR rates would intercept at around ~115 K if extrapolation to higher temperatures were physically meaningful. Assuming that spin relaxation in the initially excited Franck−Condon state of the probe molecule is due to the coupling of the solvent's structural dynamics to the rotational motion of the solute makes a potential intercept of the OR (or MER) trace with that of SLR extremely doubtful. If the rotational mobility (librational motions due to hydrodynamic and dielectric changes of the solvent cage upon excitation) is the basis for spin relaxation in viscous solution, then it is more likely that SLR rates will increase faster than thermally activated rates with increasing temperature and gradually approach the temperature dependence of OR (and MER). Because SLR is, by a factor of ~100, faster than MER and OR in the glass-transition range, the rotational mechanisms responsible for SLR are not directly observable through an effect on OR or through an effect on solvation. To test the notional prediction of the temperature dependence of k_s, measurements with a higher time resolution at higher temperatures are required, which cannot be performed with the present apparatus whose time resolution is ultimately limited by the dead time of a mechanical chopper (0.9 μs) used to separate the prompt fluorescence from the phosphorescence.

It is evident by the temperature dependence of the inverse viscosity in Figure 14 that OR and MER of the solute are based on reorientation mechanisms that are strongly linked to the structural relaxation of the solvent. The fact that the traces of OR rates and MER rates are, in good approximation, parallel shows that both relaxation phenomena are based on reorientational mechanisms whose physical natures are very similar, if not the same. This result supports the findings of Wang and Richert,[54] who were able to measure the time-dependent anisotropy ($\propto f_{rot}$) and the Stokes correlation function $C(t)$ for the same set of data using different aza-aromatics in several solvents. Reference 54 also reports reproducible differences of the characteristic solvation time, τ_{sol}, when derived from $C_\perp(t)$ and $C_\parallel(t)$ (measured with $\kappa = 90°$ and 0°, respectively). In that context, τ_{sol} was also shown to be dependent on the quantization of the transition dipole moment of the solute molecule. This important result by Wang and Richert supports our previous assumption in ref 2 that OR is expected to possess faster components of a librational nature: (i) very fast partial OR responsible for SLR (c-OR), (ii) slower partial OR leading to complete solvation (b-OR), and (iii) slow complete OR causing full phosphorescence depolarization (a-OR).[2,56] MER can, hence, be interpreted as a fast component of rotational diffusion with a small amplitude, that is, b-OR. c-OR has not yet been observed directly.

Yang and Richert[54] established criteria which predict the degree to which a-OR can be described by a single exponential.

(i) If the size relation of solute and solvent molecules, which is estimated via the corresponding molecular masses, satisfies ($m_{solute}/m_{solvent}$) > 1.3, a-OR can be described by a single exponential: this is the case for PZ in all alkanes studied here and for QX in 3MP, which corroborates this criterion.

(ii) If the ratio of τ_r/τ_{sol} is larger than 20, single exponential behavior of a-OR is expected: even though we only measured τ_{sol} for PZ in 2,3DMP at two temperatures we evaluated the ratios k_e/k_r. For QX in 3MP, we found $k_e/k_r \approx 19$, which is much smaller than a value of 50 reported in ref 45. This discrepancy is probably due to k_e not representing the correct absolute time scale of solvation. However, because the ratios k_e/k_r found for PZ in 3MP, 2,3DMP, and 3MP/IP were ≈20, 28, and 40, respectively, we still believe criterion "ii" to be confirmed by our measurements because only single exponential behavior was observed for a-OR.

4. Conclusions

SLR rate coefficients of PZ and QX in the first excited triplet state were determined in zero magnetic field by detecting the time-dependent $T_1 \rightarrow S_0$ phosphorescence without saturating a resonance transition between two triplet substates. It was shown that SLR rates are solvent-dependent in viscous solution above the glass-transition temperature; below T_g SLR becomes solvent-independent. This showed that SLR is dependent on structural properties (e.g., the viscosity) of the solvent, which influence the reorientational properties of the solute. A fast OR mechanism immediately related to SLR could, however, not be directly observed because SLR is 2−3 orders of magnitude faster than solvation dynamics and complete OR at a given temperature. SLR below T_g will be discussed in an upcoming paper.[14]

The time-dependent phosphorescence depolarization was found to be well-described by a single exponential. Complete OR rates follow a VFT law in the highly viscous regime above the glass-transition temperature and can be classified as a slow α-process. The main difference in the OR behavior of PZ and QX is sufficiently well-explained on the basis of the mechanical aspects of the solute−solvent system alone, assuming slip boundary conditions for an asymmetrically shaped rotational ellipsoid representing the solute molecule. Dielectric effects play, at best, a minor role for complete OR in the present study, which is owing to the exclusive use of non-dipolar liquids.

Solvation of PZ in 2,3DMP was measured through the time-dependent red shift of the 0,0 band of the phosphorescence at 96 and 99 K. The Stokes correlation function was described by a stretched exponential with $\beta_{sol} = 0.53$, and corresponding characteristic solvation times were estimated. We showed that the crude way of probing solvation dynamics through the time-dependent measurement of the phosphorescence in a turning point of the spectrum with high spectral resolution yields a relative measure of the solvation time scale. The corresponding rate coefficients seem to exhibit the same temperature dependence as solvation times that were established via the dynamic red shift of the spectrum in a temperature range that depends on the ratio of the triplet lifetime and the solvation time. The relation of solvation and OR is in agreement with recently published data.[45,54]

Acknowledgment. We are very grateful to Prof. Dr. J. Troe for always supporting our work and his continued interest in our research. We would like to thank Prof. Dr. N. Karl (University of Stuttgart) for providing us with zone-refined QX. Support by the German Research Council (DFG, Sonderforschungsbereich 93, Photochemie mit Lasern) is also gratefully acknowledged.

References and Notes

(1) Buckley, C. D.; McLauchlan, K. A. *Mol. Phys.* **1985**, *54*, 1.
(2) Nickel, B.; Ruth, A. A. *J. Phys. Chem.* **1991**, *95*, 2027.
(3) Antheunis, D. A.; Schmidt, J.; van der Waals, H. J. *Chem. Phys. Lett.* **1970**, *6*, 255.
(4) Antheunis, D. A.; Schmidt, J.; van der Waals, H. J. *Mol. Phys.* **1974**, *27*, 1521.
(5) Winscom, C. J.; Dinse, K. P.; Möbius, K. In *Magnetic Resonance and Related Phenomena, Proceedings of the XIXth Congress Ampère 1976*; Brunner, H., Hausser, K. H., Schweitzer, D., Eds.; Group Ampère: Heidelberg, 1976; p 413.
(6) Kohmoto, T.; Fukuda, Y.; Kuroda, R.; Hashi, T. *Chem. Phys. Lett.* **1985**, *119*, 438.
(7) Schmidt, J. Spin-Lattice and Spin-Spin-Relaxation Processes in Photo-Excited Triplet States in Molecular Crystals. In *Relaxation Processes in Molecular Excited States*; Fünfschilling, J., Ed.; Kluwer Academic Publishers: Dordrecht, The Netherlands, 1989; p 3.
(8) Lombardi, J. R.; Raymonda, J. W.; Albrecht, A. C. *J. Chem. Phys.* **1964**, *40*, 1148.
(9) Miller, L. J.; North, A. M. *J. Chem. Soc., Faraday Trans. 2* **1975**, *71*, 1233.
(10) Rutherford, H.; Soutar, I. *J. Polym. Sci., Polym. Phys. Ed.* **1977**, *15*, 2213.
(11) Ruth, A. A.; Lesche, H.; Nickel, B. *Z. Phys. Chem.* **2005**, to be submitted for publication.
(12) Richert, R. *Chem. Phys. Lett.* **1990**, *171*, 222.
(13) Richert, R. *J. Chem. Phys.* **2000**, *113*, 8404.
(14) Ruth, A. A.; Nickel, B. *J. Phys. Chem. A* **2005**, to be submitted for publication (part 2).
(15) We assume triplet−triplet annihilation and quenching processes to be negligible.
(16) Strongly selective ISC, $S_1 \rightsquigarrow T_{1i}$, from the first excited singlet state leading to extreme differences in the population of the three triplet substates, T_{1i} ($i = x, y, z$), is referred to as OSP.
(17) Asano, K.; Aita, S.; Azumi, T. *J. Chem. Phys.* **1983**, *87*, 3829.
(18) Tao, T. *Biopolymers* **1969**, *8*, 609.
(19) Perrin, F. *J. Phys. Radium* **1934**, *5*, 497.
(20) Memming, R. *Z. Phys. Chem. (Munich)* **1961**, *28*, 168.
(21) Dörr, F. Polarized Light in Spectroscopy and Photochemistry. In *Creation and Detection of the Excited State*; Lamola, A. A., Ed.; Dekker: NewYork, 1971; Vol. 1, part A, p 53.
(22) Nickel, B. *J. Lumin.* **1989**, *44*, 1.
(23) Richert, R.; Wagener, A. *J. Phys. Chem.* **1991**, *95*, 10115.
(24) The cuvette can be moved horizontally and vertically as well as rotated about a vertical axis in steps of 90°. Therefore, photochemical degradation of the sample is roughly 100 times slower than it is with an immobile sample.
(25) Ruth, A. A. Dissertation, University of Göttingen, Göttingen, Germany, 1992.
(26) The periodical changes of the polarization degree coincide with the vibronic contour bands of the phosphorescence spectrum. The minima of P are at wavenumbers $\tilde{\nu}_n(P_{min}) \approx 32\,470 - (n \times 1400)\ cm^{-1}$, with $n = 1, ..., 4$.
(27) Schmidt, J.; Antheunis, D. A.; van der Waals, H. J. *Mol. Phys.* **1971**, *22*, 1.
(28) Schwoerer, M. *17. Congress Ampère, Proc. Col. Ampère*; Hovi, V., Ed.; North-Holland Publishing: Amsterdam, 1973; Vol. 17, p 143.
(29) Zallen, R. *The Physics of Amorphous Solids*; Wiley-Interscience: New York, 1983.
(30) Gillies, R.; Spendel, W. U.; Ponte Goncalves, A. M. *Chem. Phys. Lett.* **1979**, *66*, 121.
(31) Feofil, P. P. *The Physical Basis of Polarized Emission*; Consultants Bureau: New York, 1961.
(32) Förster, T. *Fluoreszenz organischer Verbindungen*; Vandenhoeck & Ruprecht: Göttingen, 1951.
(33) Vogel, H. *Phys. Z.* **1921**, *22*, 645. Fulcher, G. S. *J. Am. Ceram. Soc.* **1925**, *6*, 339. Tammann, G.; Hesse, W. *Z. Anorg. Allg. Chem.* **1926**, *156*, 245.
(34) We refer to T_g as the temperature at which the solvent's viscosity η reaches 10^{15} mPa s (= 10^{15} cP).
(35) Murthy, S. S. N. *J. Chem. Soc., Faraday Trans. 2* **1989**, *85*, 581.
(36) Ruth, A. A.; Nickel, B.; Lesche, H. *Z. Phys. Chem.* **1992**, *175*, 91.
(37) Perrin, F. *J. Phys. Radium* **1936**, *7*, 1.
(38) For stick boundary conditions to hold, the tangential velocities of the solute and the solvent molecules at the solute−solvent interface are assumed to be the same.
(39) One of the transition moments involved (either that for emission or that for absorption) must be polarized along the rotational axis of the ellipsoid for eq 11 to hold.
(40) Hirata, Y.; Tanaka, I. *Chem. Phys. Lett.* **1976**, *43*, 568. Narva, D. L.; McClure, D. S. *Chem. Phys.* **1981**, *56*, 167.
(41) Kummer, F.; Zimmermann, H. *Ber. Bunsen-Ges. Phys. Chem.* **1967**, *71*, 1119. El-Sayed, M. A.; Brewer, R. G. *J. Chem. Phys.* **1963**, *39*, 1623. Jordan, A. D.; Fischer, G.; Rokos, K.; Ross, I. G. *J. Mol. Spectrosc.* **1973**, *45*, 173.
(42) If no tangential force is exerted on the rotating molecule by the solvent, the boundary condition is known to be "slip". Spheres experience zero friction for slip conditions.
(43) Hartmann, R. S.; Alavi, D. S.; Waldeck, D. H. *J. Phys. Chem.* **1991**, *95*, 7872.
(44) Sension, R. J.; Hochstrasser, R. M. *J. Chem. Phys.* **1993**, *98*, 2490.
(45) Yang, M.; Richert, R. *Chem. Phys.* **2002**, *284*, 103.
(46) Rössler, E. *Ber. Bunsen-Ges. Phys. Chem.* **1990**, *94*, 392.
(47) Rössler, E. *J. Chem. Phys.* **1990**, *92*, 3725.
(48) Shahriari, S.; Mandanici, A.; Wang, L.-M.; Richert, R. *J. Chem. Phys.* **2004**, *121*, 8960.
(49) Maroncelli, M.; Fleming, G. R. *J. Chem. Phys.* **1987**, *86*, 6221.
(50) Nagarajan, V.; Brearley, A. M.; Kang, T.-J.; Barbara, P. F. *J. Chem. Phys.* **1987**, *86*, 3183.
(51) Wagener, A.; Richert, R. *Chem. Phys. Lett.* **1991**, *176*, 329.
(52) Maroncelli, M.; McInnis, J.; Fleming, G. R. *Science* **1989**, *243*, 1674.

(53) Oppenheim, I. Linear Response Theory and Spin-Relaxation. In *Electron Spin Relaxation in Liquids*; Muus, L. T., Atkins, P. W., Eds.; Plenum Press: New York, 1972; p 109.

(54) Wang, L.-M.; Richert, R. *J. Chem. Phys.* **2004**, *120*, 11082.

(55) A more accurate description of the time-dependent phosphorescence would be based on the dynamics of the red shift of the $T_1 \rightarrow S_0$ spectrum in conjunction with the shape of the emission band in the vicinity of the detection wavelength. This time-dependent convolution of the spectral shape with a stretched exponential (eq 17) is then subject to the overall triplet decay. Because solvation is theoretically never finished during the lifetime of the triplet and because back extrapolation to the intensity at the time of excitation becomes virtually impossible, boundary conditions cannot be established and the parameters in a fit, thus, yield meaningless values. Equation 18 only holds in a temperature regime where solvation is (i) fast enough, so that red shift of the spectrum becomes virtually negligible during the triplet lifetime ($k_e \gg k_0$), and (ii) slow enough, so that a small part of a stretched exponential can be sufficiently well-represented by a simple exponential at a given time resolution and experimental noise. Note that in all measurements the first few microseconds after excitation were always cut off by a chopper used in the experiment.[2]

(56) In ref 2 the three components were referred to as α-OR, β-OR, and γ-OR.